Carbon nanotube tori under external fields

C. G. Rocha,[1] M. Pacheco,[2] Z. Barticevic,[2] and A. Latgé[1,*]
[1]*Instituto de Física, Universidade Federal Fluminense, 24210-340 Niterói-RJ, Brazil*
[2]*Departamento de Física-Universidad Técnica, F. Santa Maria, Casilla 110-V, Valparaiso, Chile*
(Received 3 February 2004; revised manuscript received 20 April 2004; published 3 December 2004)

We address here a theoretical study on the role played by external magnetic and electric fields on the electronic properties of toroidal carbon nanotubes. A single-π band tight-binding calculation is adopted and real-space renormalization techniques are used to obtain electronic energy spectra. Induced gap modulations are found by applying electric and magnetic fields in different spatial configurations. By changing electronic and transport properties of the annular structure with the fields, metal-insulator transitions are allowed for particular tube geometries an field intensities.

DOI: 10.1103/PhysRevB.70.233402 PACS number(s): 73.63.Fg, 73.22.−f, 73.61.Wp

A large number of applications of carbon nanotubes (CN's) has been recently suggested and even observed, based mainly on the peculiar physical property of behaving as metal or semiconducting materials.[1] Metal-insulator transitions in CN devices may occur, for instance, due to spatial induced radial deformations perpendicular to the tube axis.[2] Depending on the particular symmetry broken, potential barriers are formed and may change completely the electron transmission properties. In that sense, carbon nanotubes may be used as nanometric electromechanical switches. Other mechanisms are also used to induce electronic transition such as the application of transversal electrical fields on straight tubes.[3,4] The relative position between deposited CN's and substrates may be controlled using a local electric field generated by electrodes. Opening and closing of the electronic gap have been found to occur in metallic and semiconducting zigzag tubes,[5,6] respectively. Also, under high electric field conditions, typical nanojunctions may be formed by fusion of two adjacent tubes.[7]

Homogeneous magnetic fields threading the annular system such as the CN's are used for many applications due to important changes on the electronic structure imposed by varying the magnetic flux.[8] For instance, magnetoconductance measurements and theoretical calculations have shown the presence of the Aharonov-Bohm (AB) oscillations due to the phase shift of the electronic wave function induced by the magnetic field.[9,10] The combination of both magnetic and electrostatic potentials may certainly be investigated since it provides alternative schemes of quantum interference of electron waves.[11] Besides the straight tubes, other annular geometries have been observed during the synthesis processes of CN's,[12] called toroidal carbon nanotubes (TCN's). The formation of those molecules has been attributed to the balance between van der Waals attraction between the two ends of the strip mediated by catalytic particles, acting as solder, and strain energies.[13] In transport measurements, carbon rings and tubes are usually placed in metal electrodes, oxide substrate, gate potentials, and magnetic fields.[14,15] Theoretically, a TCN may be viewed as a bent graphite sheet with simultaneously transversal and longitudinal periodical boundary conditions. Perturbations induced by impurities, vacancies, and magnetic fields, on the electronic properties of TCN's have been investigated.[16] It was shown that the corresponding local density of states exhibit a sequence of well-defined peaks, typical of finite systems which are shifted under a magnetic field. The central gap size of a TCN is periodically modulated by increasing the magnetic flux threading the torus cross section, highlighting the *AB* oscillations.[17] By adding electric and magnetic fields one may certainly induce further changes in the electronic properties of the TCN's.

In this work, we analyze electronic properties of TCN's under external fields applied in the Hall-field configuration shown in Fig. 1(a) (magnetic field *B*, and electric field *E*, perpendicular and parallel to the torus plane, respectively[18]), and also considering both fields applied perpendicularly to the torus plane, as depicted in Fig. 1(b). We follow a single π-band tight binding approach and use the Peierls-phase approximation[9,10] to consider the magnetic field. In this picture, a phase is added to the hopping integrals of the tight binding Hamiltonian, which depends on the magnetic flux ϕ and is given in terms of a quantum flux $\phi_0 = hc/e$. The effect of the electric field is included into the on-site energies of the carbon atoms, following a linear interpolation for the potential energy difference along the cross section, given by *V*. The Hamiltonian of the CN is entirely treated in the real space and may be written as

$$H = \sum_{i,\alpha} \epsilon_i^{\alpha}(V) c_i^{+\alpha} c_i^{\alpha} + \sum_{i,j}^{\alpha,\beta} \gamma_{i,j}^{\alpha,\beta}(B) c_i^{+\alpha} c_j^{\beta}, \qquad (1)$$

with α and β denoting the positions of the carbon atoms displayed along two first neighbor rings, named *i* and *j*. The diagonal energy is given by $\epsilon_i^{\alpha}(V) = \epsilon_{i,\alpha}^{0} - V/2 \cos(\theta_i^{\alpha})$, equal to $\epsilon_{i,\alpha}^{0}$, for null electric field and with θ_i being the angle defined by the electric field direction and the atomic position along the CN or torus circumference, depending on the electric field configuration. $\gamma_{i,j}^{\alpha,\beta}(B)$ corresponds to the hopping energies, written within the Peierls phase approximation.[9,10]

As the usual renormalization techniques adopted in the Green function formalism[19,20] become more complex in the Hall-field configuration, we numerically diagonalize the tight binding Hamiltonian matrices. Within the adopted single π-band model the results are restricted to the energy range near the Fermi level. Also, no curvature effects are considered in the present description. For the sake of simplicity we analyze achiral torus such as zigzag/armchair (A/Z) and

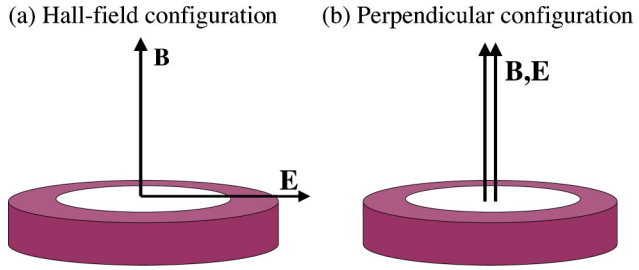

FIG. 1. Schematic view of the (a) Hall-field and (b) perpendicular-field configurations used in the discussion.

armchair/zigzag (Z/A), denoted as $(n,0,p,p)$ and $(n,n,p,0)$, respectively. Notice that n is associated with the nanotube radius composing the torus whereas $p=N(A/Z)$ and $N/2(Z/A)$, N being the number of connected rings, which defines the torus radius R. Although the description of realistic tori requires $p \gg n$, the main features of the effects of electric and magnetic fields on the TCN energy spectra may be seen even considering TCN's with smaller radii. Being a finite nanostructure, the corresponding spectra are completely discrete and therefore the effects produced by the external fields may be investigated with more clarity.

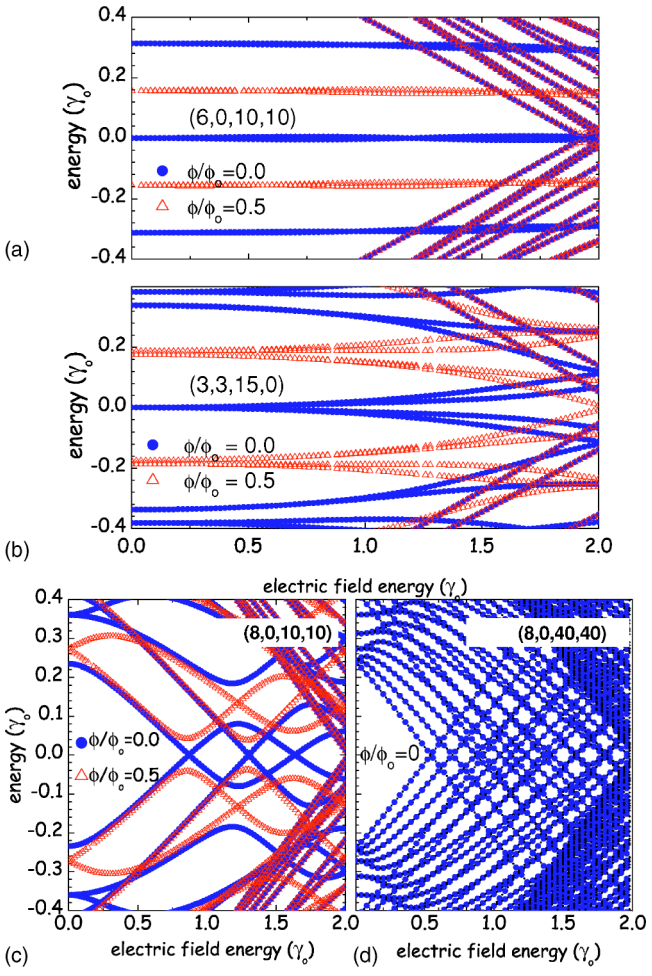

FIG. 2. Energy spectra as a function of the electric field energy (Hall configuration) for (a) (6,0,10,10), (b) (3,3,15,0), (c) (8,0,10,10), and (d) (8,0,40,40) TCN's. Full circles and open triangles correspond to $\phi/\phi_0=0$ and 0.5, respectively.

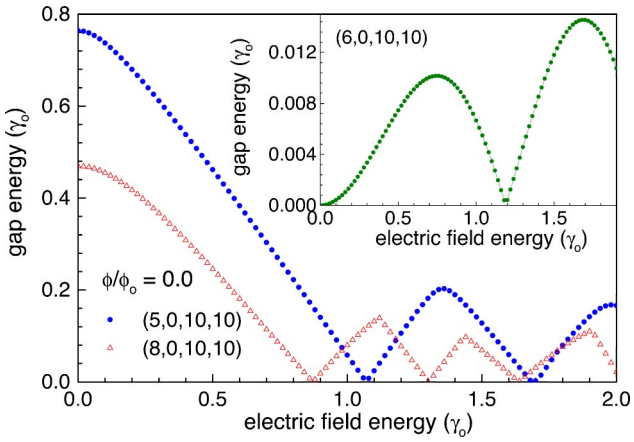

FIG. 3. Energy gap dependence on the effective electric field intensity for the (5,0,10,10) and (8,0,10,10) TCN's and for the (6,0,10,10) in the inset. All the results are for $\phi/\phi_0=0$.

Three TCN's are considered as Z/A examples, (6,0,10,10), (8,0,10,10), and (8,0,40,40), whereas a (3,3,15,0) A/Z is chosen. The corresponding TCN spectra for the Hall configuration are shown in Fig. 2 as functions of the electric field energy. The results are for $\phi/\phi_0=0$ and 0.5 [except Fig. 2(d)]. The electric field energy is given in units of the hopping integral γ_0 ($\approx$3.0 eV). Notice that both field intensities (magnetic and electric) are scaled with the torus radius since we deal with magnetic flux values (proportional to R^2) and with electric-field energies (proportional to R). For the small R, therefore, the energy range considered in the figures correspond to an electric field up to $\approx 10^4$ kV/cm. For the larger (8,0,40,40) TCN [see Fig. 2(d)], one clearly notices that, as expected, the gap closing occurs at a smaller electric field energy than for the (8,0,10,10) TCN, corresponding to an electric field of the order of 10^3 kV/cm, comparable to experimental realizations.[8,21] An increasing number of discrete states is evident, making the study of the evolution of the electronic states with the electric field also more difficult to perform.

For the (6,0,10,10) Z/A torus [Fig. 2(a)], the states near the Fermi level present a very weak dispersion with the electric field energy whereas a different picture is evidenced for the (8,0,10,10) [Fig. 2(c)]. The lost symmetry, induced by the electric fields, is exhibited by the degeneracy lift of some levels in the studied spectra. A kind of metal-insulator transition, for null magnetic flux, is also apparent in the TCN's spectra at specific electric field values when electronic bands cross at the Fermi level ($\epsilon_F=0$). For a certain magnetic field intensity, the bands are shifted and interbands crossing at the Fermi energy stop happening, as a consequence of destructive interference of the electronic wave functions.

The energy gaps, defined as the energy distance between the HOMO and LUMO states, are shown in Fig. 3 for three Z/A TCN's ($n=5$, 6, and 8; $p=10$) and for $\phi/\phi_0=0$. The oscillation amplitudes are considerably greater for the case of the (5,0,10,10) and (8,0,10,10) TCN's than for the (6,0,10,10). Due to the weak dispersion of the energy levels

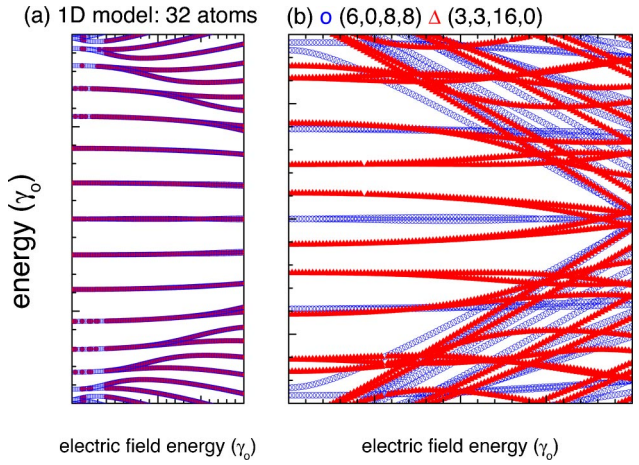

FIG. 4. Dependence of the electronic states with the electric field energy for (a) an one-dimensional ring composed of 32 atoms and for (b) (6,0,8,8) and (3,3,16,0) TCN's, given by open circles and up triangles, respectively.

around ϵ_F in the spectra of the (6,0,10,10) tube, the gap magnitude is very small ($\approx 0.01\gamma_0$). As the electric field increases some excited states cross the Fermi level allowing extra gap modulations besides those originated by the behavior of the HOMO and LUMO states. A superposed effect is clearly observed in the curves related to the (8,0,10,10) and (5,0,10,10) TCN's.

A strictly one-dimensional ring model is used to highlight the effects of in-plane electric fields on the electronic states. According to the adopted model, the energy dispersion for an atomic ring composed of M atoms, in the absence of external fields, is given by $\epsilon_n = -2\gamma \cos(2\pi n/M)$, n being an integer number, $n = 1, 2, \ldots, M$. The corresponding energy spectra is hence composed of $M/2-1$ $[(M-1)/2]$ degenerate states and two (one) nondegenerate ones for even-folded (odd) rings. As an in-plane electric field is turned on, the electronic states split, lifting the double degeneracy due to the nonequivalence of the atomic energies, as it is shown in Fig. 4(a), for a one-dimensional (1D) loop with $M = 32$. The effect of the atomic distribution across the circumference on the

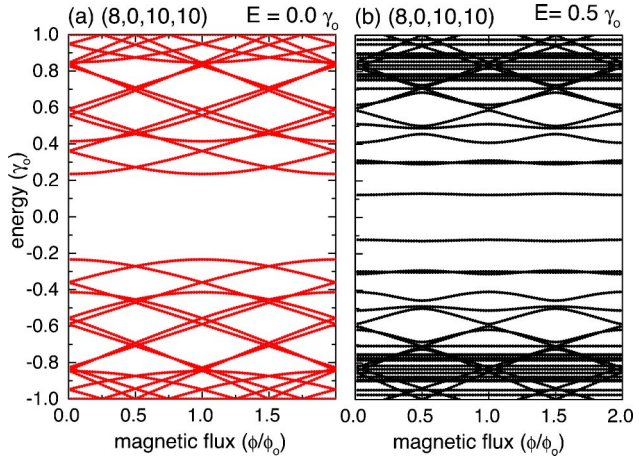

FIG. 5. Energy spectra versus magnetic flux for a (8,0,10,10) TCN and (a) zero and (b) 0.5 γ_0 electric field.

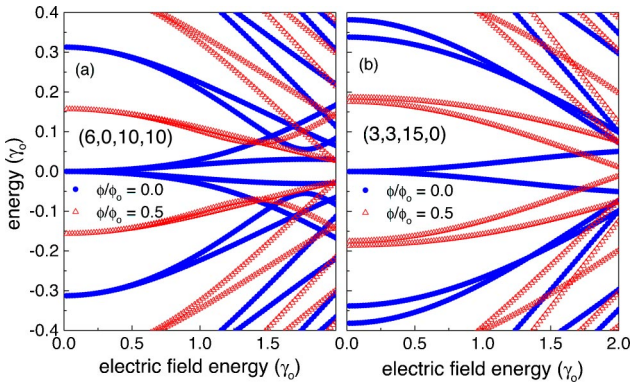

FIG. 6. Energy spectra versus electric field energy for (a) (6,0,10,10) and (b) (3,3,15,0) TCN's and fixed magnetic flux adopting parallel field configuration.

energy spectrum is also investigated by choosing two different arrays, simulating strictly one-dimensional armchair and zigzag virtual tubes, i.e., made solely by a single ring. As expected by the geometric aspect, the results are almost identical, exhibiting small differences only for the states at the Fermi level. The energy spectra of two TCN's, both with 32 carbon atoms displayed along the plane of the tori and equal number of total atoms (192), are shown in Fig. 4(b) [(6,0,8,8) and (3,3,16,0)]. The role played by the CN radii on the energy spectra is clearly noticed even for zero electric field, showing that the microscopic details of the atomic distribution across the structures are actually important. Moreover, as the electric field is turned on, the difference increases, and it is possible to distinguish between armchair and zigzag configurations. The general results emphasize the idea that electrical responses may be used in structural characterization of CN's and TCN's.

By varying the intensity of the magnetic field threading the TCN's one induces the well known *AB* phenomena, as shown in Fig. 5(a) for a (8,0,10,10) TCN spectra in the absence of electric field. Similar to what happens to a very thin GaAs-semiconducting ring,[18] an electric field applied in the Hall configuration destroys the oscillating features of the low lying states, due to the field-induced localization. The oscillatory response is still exhibited in the energy region of the excited states, for which the delocalization nature of the

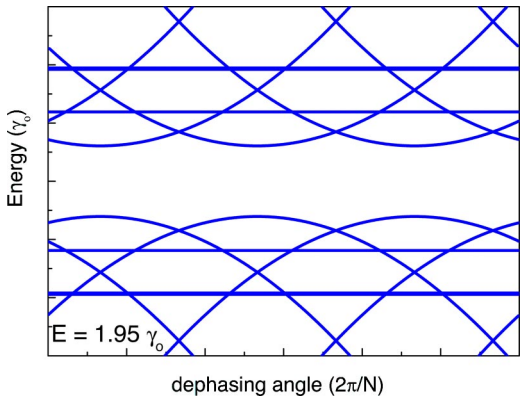

FIG. 7. Dependence of the energy spectra on the dephasing angle for a (8,0,10,10) TCN and an electric field equal to $1.95\gamma_0$, applied in the plane of the torus.

states allows *AB* interference pattern [see Fig. 5(b)]. The effects of both fields are independent and may be conveniently manipulated to induce electronic changes in the energy spectra.

We investigate now the electronic spectra considering the perpendicular field configuration, shown in Fig. 1(b). This configuration may be experimentally realized by displaying two capacitor planes above and below the torus.[3,4] The energy spectra for a (6,0,10,10) Z/A and a (3,3,15,0) A/Z are shown in Fig. 6. Notice that these are the same TCN's studied in the Hall-field configuration, and shown in Figs. 2(a) and 2(b). In contrast to the previously reported results, the energy spectrum for the (6,0,10,10) exhibits huge divergent dispersions as the electric field energy increases, for null magnetic flux. Additionally, four states emerge from the state $E_F=0$ whereas only two states oscillate in Fig. 2(a) around E_F, in the other field configuration. The direction of the electric field plays therefore an essential role, lifting or not the characteristic degeneracy of the states near the Fermi level. These features may be understood based on a simple analysis of the degeneracy in straight CN's.

Within a π-band tight binding picture, zigzag tubes are known to present double-degenerated bands near ϵ_F. When the electric field acts in a zigzag geometry, as it is in the case of the last configuration [see Fig. 6(a) (Z/A)], the characteristic double degeneracy of the two first bands are broken due to the new on-site energies induced by the local electric field. In the Hall field configuration, the electric field is applied in the torus plane direction, threading an armchair configuration, so no degeneracy is lifted once the two bands around E_F are nondegenerate. The same features may be observed for the A/Z torus, shown in Figs. 6(b) and 2(b). The simple discussed example points out, once more, that the electric field may be used to investigate atomic structure of the TCN's, as it is already done with STM tip mappings.

A further interesting electric-field effect is found for Z/A tori with the fields applied in the Hall configuration. By considering a dephasing angle between the electric field direction and the position of the carbon atoms along the toroid one finds a clear modification of the energy spectra deriving essentially from the lattice symmetry of the graphite sheet. Actually, for an even number of atoms along the zigzag CN, certain eigenenergies in the toroid spectrum oscillate as a function of a dephasing angle. The range and position of those particular energies, and the amplitude and period of the oscillations, may be conveniently modulated by changing the strength and direction of the electric field. This effect may be easily studied by adding an angle (ψ) in the on-site energies, to simulate a rotation, i.e., $\epsilon_i^\alpha=\cos(\theta_i^\alpha+\psi)V/2$.

An example of the dependence of the energy spectra on the dephasing angle is shown in Fig. 7 for a (8,0,10,10) TCN under an in-plane electric field of $1.95\gamma_0$. For this particular value the oscillations appear next to the main energy gap region. A detailed analysis of this effect, including analytical expressions for the oscillating energies as a function of the electric-field dephasing angle, will be presented elsewhere. CN and nanostructures, and in particular the studied toroidal tubes, may exhibit a richness of electronic properties depending upon their intrinsic geometric formation. Adding external fields, one may intentionally modify these properties and modulate their physical responses. We analyzed here the energy spectra for distinct geometries of torus under the influence of electric and magnetic fields applied in different configurations. We believe that a better understanding of the physics of carbon nanostructures, even within a simple picture such as the one adopted here, should help us to propose their use in real nanodevices.

This work was partially supported by CNPq, FAPERJ, Fondecyt 1010429 and 7010429, Iniciativa Cientifica Milenio P02-054-F, and Instituto do Milênio para Nanociências/MCT/Brazil.

*Electronic address: latge@if.uff.br

[1] J. W. Mintmire, B. I. Dunlap, and C. T. White, Phys. Rev. Lett. **68**, 631 (1992).
[2] C. J. Park, Y. H. Kim, and K. J. Chang, Phys. Rev. B **60**, 10 656 (1999); H. S. Sim, C. J. Park, and K. J. Chang, *ibid.* **63**, 73 402 (2001).
[3] X. Zhou, H. Chen, and O. Y. Zhong-can, J. Phys.: Condens. Matter **13**, L635 (2001).
[4] Y. H. Kim and K. J. Chang, Phys. Rev. B **64**, 153404 (2001).
[5] Y. Li, S. V. Rotkin, and U. Ravaioli, Nano Lett. **3**, 183 (2003).
[6] J. O'Keeffe, C. Wei, and K. Cho, Appl. Phys. Lett. **80**, 676 (2002).
[7] G. W. Ho, A. T. S. Wee, and J. Lin, Appl. Phys. Lett. **79**, 260 (2001).
[8] A. Bachtold *et al.*, Nature (London) **397**, 673 (2001).
[9] S. Roche, G. Dresselhaus, M. S. Dresselhaus, and R. Saito, Phys. Rev. B **62**, 16 092 (2000).
[10] H. Ajiki and T. Ando, J. Phys. Soc. Jpn. **65**, 505 (1996).
[11] A. van Oudenaarden, M. H. Devoret, Y. V. Nazarov, and J. E. Mooij, Nature (London) **391**, 768 (1998).
[12] J. Liu *et al.*, Nature (London) **385**, 780 (1997).
[13] R. Martel, H. R. Shea, and P. Avouris, Science **398**, 299 (1999).
[14] C. Dekker, Phys. Today **52** (5), 22 (1999).
[15] J.-O. Lee *et al.*, Solid State Commun. **115**, 467 (2000).
[16] A. Latgé *et al.*, Phys. Rev. B **67**, 155413 (2003).
[17] R. C. Haddon, Nature (London) **388**, 31 (1997).
[18] Z. Barticevic, G. Fuster, and M. Pacheco, Phys. Rev. B **65**, 193307 (2002).
[19] M. S. Ferreira, T. G. Dargam, R. B. Muniz, and A. Latgé, Phys. Rev. B **62**, 16 040 (2000).
[20] C. G. Rocha, T. G. Dargam, and A. Latgé, Phys. Rev. B **65**, 165431 (2002).
[21] H. Watanable, C. Manable, and T. Shigematsu, Appl. Phys. Lett. **78**, 2928 (2001).